thank Dr. F. S. Tham (Rensselaer) for the X-ray diffraction study of the *p*-bromobenzoate of **11**. We thank Degussa AG for a generous gift of L-proline.

Registry No. 2, 139760-48-8; **3a** (isomer 1), 139760-49-9; **3a** (isomer 2), 139760-50-2; **3b** (isomer 1), 139760-51-3; **3b** (isomer 2), 139760-52-4; **3c** (isomer 1), 139869-59-3; **3c** (isomer 2), 139869-60-6; **3d** (isomer 1), 139760-53-5; **3d** (isomer 2), 139760-54-6; **3e** (isomer 1), 139760-55-7; **3e** (isomer 2), 139760-56-8; **3f** (isomer 1), 139760-57-9; **3f** (isomer 2), 139760-58-0; **3g** (isomer 1), 139760-59-1; **3g** (isomer 2), 139760-60-4; **4a**, 139760-61-5; **4b**, 139760-62-6; **4c**, 139760-63-7; **4d**, 139760-64-8; **4e**, 139760-65-9; **4f**, 139760-66-0; **4g**, 139760-67-1; **6**, 139760-68-2; (2*R*,3*S*)-**7**, 139894-31-8; (2*S*,3*S*)-**7**, 139894-32-9; **8**, 139760-69-3; **9**, 139894-33-0; **10**, 115588-50-6; (1*S*,3*S*)-**11**, 139760-70-6; (1*R*,3*S*)-**11**, 139894-34-1; **12**, 139760-71-7; methyl 3-methoxy-2-methylbenzoate, 42981-93-1; (*S*)-2-(methoxymethyl)pyrrolidine, 63126-47-6.

Supplementary Material Available: Tables of crystal structure data, atomic coordinates, bond lengths, bond angles, anisotropic parameters, and hydrogen atom coordinates for the *p*-bromobenzoate derivative of **11** (7 pages). Ordering information is given on any current masthead page.

Synthesis and Aggregation Properties of a New Family of Amphiphiles with an Unusual Headgroup Topology

Thomas M. Stein and Samuel H. Gellman*

Contribution from the S. M. McElvain Laboratory of Organic Chemistry, Department of Chemistry, University of Wisconsin, Madison, Wisconsin 53706. *Received November 18, 1991*

Abstract: A new family of amphiphiles, derived from a rigid dicarboxylic acid headgroup unit of unusual topology, has been synthesized. The aggregation of these molecules in aqueous solution has been examined by ^{1}H NMR and dye solubilization methods. Two modes of aggregation appear to be operative within this group of amphiphiles, one determined by the headgroup and the other determined by the flexible tail. The former mode is dominant when the tail is short or nonexistent, and the latter is dominant when the tail contains six or more nonpolar atoms. The latter mode appears to be a typical micellization process, but the former is less cooperative. For the latter group of amphiphiles, comparison with literature data for a family of long chain alkyl malonate surfactants indicates that the wide, rigid headgroup, containing 16 non-carboxylate carbon atoms, has the equivalent "hydrophobic impact" on aggregation of only five CH_2 groups in the flexible tail.

Introduction

Physical studies of synthetic amphiphiles have tended to focus on molecules with a single topology: a compact polar headgroup connected to one or more flexible hydrocarbon tails.[1] This structural family is widely represented among the biologically and industrially important amphiphiles, but many other amphiphilic architectures are possible. Mukerjee, for example, has identified several structural classes of molecules that can undergo "hydrophobic association" in aqueous solution:[2] (1) species with the classical polar headgroup/nonpolar flexible tail architecture (soaps, detergents, lipids, etc.); (2) polycyclic aromatic amphiphiles that are rigid and planar (e.g., methylene blue); (3) rigid but nonplanar structures with surfaces of differing polarity (e.g., the bile acid salts); and (4) macromolecules, including proteins.

Differing aggregation behavior among these types of structures makes it clear that amphiphilic topology has a profound effect on solution behavior. Amphiphiles in the large first class tend to form discretely sized aggregates, such as micelles and vesicles.[1] Molecules in the second class, however, tend to undergo stepwise association that does not result in aggregates of discrete sizes.[3] Cholate and other steroidal members of the third class exhibit aggregation properties intermediate between those of the first two classes, showing weak cooperativity that leads to polydispersity in aggregate size.[4] Israelachvili has analyzed the effects of structural variations among species bearing a polar headgroup and at least one flexible nonpolar tail, showing that geometric packing considerations lead to a rational correlation between molecular structure and the type of aggregate formed (e.g., spherical micelles vs rod-shaped micelles vs bilayers).[5] In light of the important functions performed by amphiphilic species in diverse settings,[1] it is not surprising that exploration of new amphiphilic architectures is a subject of continuing interest.[6-11]

We are interested in an amphiphile topology that has not previously received much attention in synthetic systems: rigid structures with two discrete faces, one of which is polar and the other nonpolar. The bile salts, which possess unusual aggregation, solubilization, and membrane-modification properties,[4] have a related architecture; one face of the rigid steroid skeleton is polar, because of the hydroxyl groups, and the other is nonpolar. The bile salts differ somewhat from our structural prescription, how-

(1) For leading references, see: (a) Myers, D. *Surfactant Science and Technology*; VCH Publishers, Inc.: New York, 1988. (b) Fendler, J. H. *Membrane Mimetic Chemistry*; John Wiley & Sons: New York, 1982. (c) Lindman, B.; Wennerström, H. *Top. Curr. Chem.* **1980**, *87*, 1. (d) Mukerjee, P.; Mysels, K. J. *Natl. Stand. Ref. Data Ser., Natl. Bur. Stand.* **1971**, No. 36.

(2) Mukerjee, P. *J. Pharm. Sci.* **1974**, *63*, 972.

(3) Mukerjee, P.; Ghosh, A. K. *J. Am. Chem. Soc.* **1970**, *92*, 6403.

(4) (a) Roda, A.; Hofmann, A. F.; Mysels, K. J. *J. Biol. Chem.* **1982**, *258*, 6362. (b) Mukerjee, P.; Moroi, Y.; Murata, M.; Yang, A. Y. S. *Hepatology* **1984**, *4*, 61S.

(5) Israelachvili, J. N.; Marcelja, S.; Horn, R. G. *Q. Rev. Biophys.* **1980**, *13*, 121.

(6) Menger and co-workers have examined the aggregation properties of a number of amphiphiles with unusual topologies; see: (a) Menger, F. M.; Whitesell, L. G. *J. Org. Chem.* **1987**, *52*, 3793. (b) Menger, F. M.; Littau, C. A. *J. Am. Chem. Soc.* **1991**, *113*, 1451.

(7) Jolicoeur et al. have studied the aggregation of a series of potassium alkylcarboxylates, the hydrocarbon moieties of which varied in compactness from linear chains to polycyclic structures (e.g., adamantyl). Jolicoeur, C.; Paquette, J.; Lavigne, Y.; Zana, R. In *Solution Behavior of Surfactants*; Mittal, K. L., Fendler, E. J., Eds.; Plenum Press: New York, 1982; Vol. 2, p 388.

(8) Attwood has examined aggregation of drug molecules possessing varied amphiphilic structures, see: Attwood, D. *J. Phys. Chem.* **1976**, *80*, 1984 and references therein.

(9) Engberts and co-workers have explored the relationship between amphiphile structure and surfactant morphology among 1,4-dialkylpyridinium halides. (a) Nusselder, J.-J. H.; Engberts, J. B. F. N. *J. Am. Chem. Soc.* **1989**, *111*, 5000. (b) Nusselder, J.-J. H.; Engberts, J. B. F. N. *J. Org. Chem.* **1991**, *56*, 5522.

(10) It has been suggested that certain "cascade molecules" may be thought of as "unimolecular micelles"; see: Newkome, G. R.; Yao, Z.; Baker, G. R.; Gupta, V. K. *J. Org. Chem.* **1985**, *50*, 2003.

(11) For studies of the aggregation of small uncharged molecules in aqueous solution, see: (a) Desrosiers, O.; Van Dinter, T.; Saunders, J. K. *Can. J. Chem.* **1984**, *62*, 56. (b) Zana, R.; Michels, B. *J. Phys. Chem.* **1989**, *93*, 2643.

0002-7863/92/1514-3943$03.00/0

Scheme I

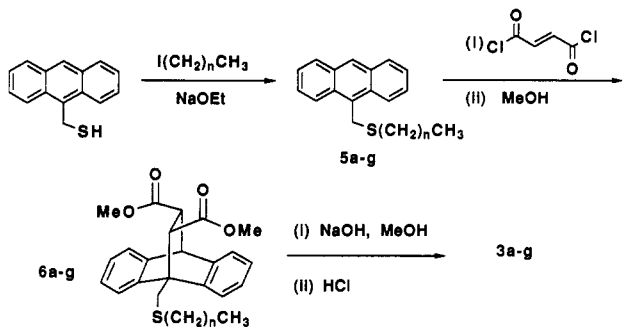

ever, because the carboxylate group extends approximately laterally from the mean plane of the rigid skeleton.

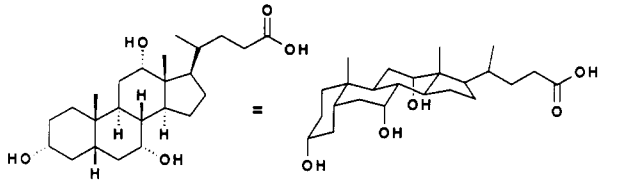

Cholic Acid

The Diels–Alder adduct of fumaric acid and anthracene (**1**)[12] achieves the unusual amphiphilic topology in which we are interested. In its doubly ionized form, **1** has a concave nonpolar face defined largely by the surfaces of the aromatic rings that are distal to the carboxylate-bearing bridge and a convex polar face dominated by the two carboxylate groups. We describe here the preparation and characterization of a new series of amphiphiles, including the disodium salts of **2**, **3a–g**, and **4**, for which the dibenzobarrelane skeleton of **1** serves as the key structural element.[13,14]

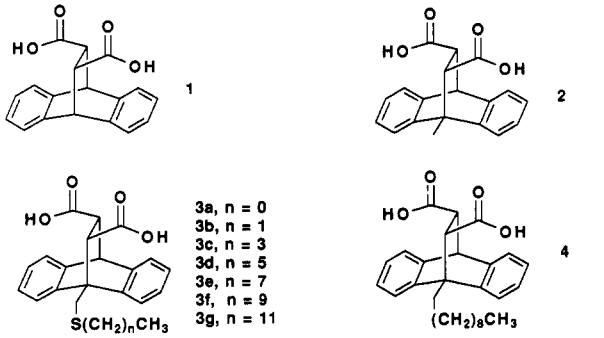

Results and Discussion

Synthesis. Diacid **2** was prepared by Diels–Alder reaction between 9-methylanthracene and fumaryl dichloride followed by a methanol quench and subsequent saponification. Diacids **3a–g** were synthesized as indicated in Scheme I. 9-Anthracenylmethanethiolate was allowed to react with a series of alkyl halides, and the resulting thioethers (**5a–g**) were subjected to Diels–Alder reaction with fumaryl dichloride, followed by methanolysis and saponification. The synthesis of diacid **4** (the analogue of **3e** bearing an all-carbon tail) began with the alkylation of the enolate of 9-acetylanthracene with octyl iodide (Scheme II). The ketone produced (**7**) was reduced with $LiAlH_4$, and the resulting alcohol

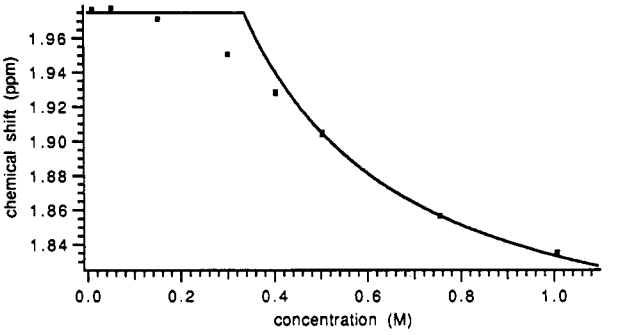

Figure 1. ^1H NMR chemical shift of the methyl group at C9 of the disodium salt of **2** as a function of amphiphile concentration (30 °C). The smooth curve was generated by a fit to eqs 1 and 2, as described in the text. The derived CAC is 320 mM.

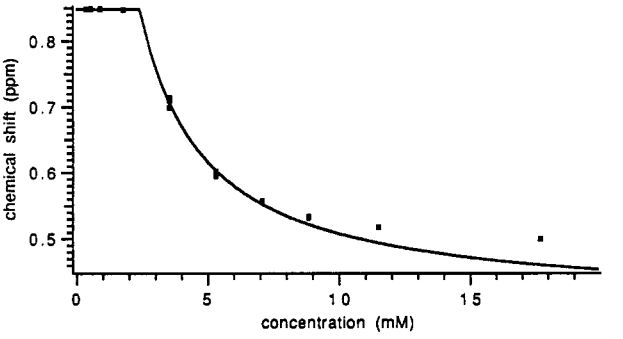

Figure 2. ^1H NMR chemical shift of the terminal methyl group on the alkyl chain of the disodium salt of **3g** as a function of amphiphile concentration (30 °C). The smooth curve was generated by a fit to eqs 1 and 2, as described in the text. The derived CAC is 2.2 mM.

Scheme II

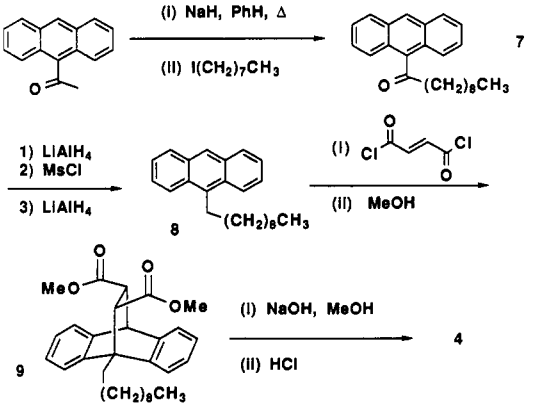

was mesylated and further reduced with $LiAlH_4$ to produce 9-decylanthracene (**8**). Treatment of **8** with fumaryl dichloride followed by reaction with MeOH produced diester **9**, the saponification of which yielded **4**. Disodium salts of **1–4** were generated by the addition of 2 equiv of aqueous NaOH to suspensions of the diacids in water.[15] No attempt was made to resolve the enantiomers of these synthetic amphiphiles.

Unlike all other amphiphiles in the series **1–4**, the disodium salt of **3g** was not water-soluble at room temperature. This disodium salt could be dissolved at higher temperatures (the Krafft

(12) Bachmann, W. E.; Scott, L. B. *J. Am. Chem. Soc.* **1948**, *70*, 1458.

(13) The antidepressant maprotiline contains a dibenzobarrelane unit; a flexible alkyl chain attached to one of the bridgehead carbons bears an amine. The aggregation of maprotiline·HCl has been examined: Thoma, K.; Albert, K. *Pharm. Acta Helv.* **1979**, *54*, 330.

(14) Dougherty and co-workers have prepared macrocycles containing two dibenzobarrelane or dibenzobarrelenedicarboxylate subunits as receptors for hydrophobic guests. These macrocycles have been reported to aggregate in aqueous solution: (a) Petti, M. A.; Shepodd, T. J.; Dougherty, D. A. *Tetrahedron Lett.* **1986**, *27*, 807. (b) Petti, M. A.; Shepodd, T. J.; Barrans, R. E.; Dougherty, D. A. *J. Am. Chem. Soc.* **1988**, *110*, 6825.

(15) The disodium salts of **1–4** were stored in a dessicator as lyophilized powders. When these materials were redissolved in water, the solution pH was always >9. Titration of diacid **1** (concentration ≤0.1 M) indicates that the carboxyl group pK_a values are approximately 4.5 and 5.5; therefore, at the high pH values measured for the solutions containing the disodium salts, we assume that both carboxylate groups of each amphiphile molecule are essentially completely deprotonated. In a representative case (**3e**), the solution pH was monitored as a function of amphiphile concentration during a CAC determination. For the highest concentration sample (61 mM), the pH was 11.4, and for the lowest concentration sample (1.8 mM), the pH was 10.2.

point was determined to be 45 °C), and the precipitation of disodium **3g** from solutions cooled to 30 °C was slow enough that aggregation studies could be carried out by ^{1}H NMR spectroscopy at this temperature, as described below.

Characterization of Aggregation Behavior. Amphiphile aggregation may be characterized by monitoring any of a number of physical parameters as a function of amphiphile concentration.[1] We used the concentration dependence of ^{1}H NMR chemical shifts as our primary analytical tool, and we checked our results for several compounds by a dye solubilization method.

The disodium salts of all diacids **1–4** showed concentration-dependent shifts in at least some of their ^{1}H NMR resonances in aqueous solution. For the disodium salts of **2**, **3a–g**, and **4**, the resonance of the terminal methyl group was a particularly convenient probe. Data for the disodium salt of **2** are shown in Figure 1, and data for the disodium salt of **3g** are shown in Figure 2. (The smooth curves in Figures 1 and 2 are derived from a treatment of the data based on the pseudo-phase-separation model, as discussed below.) Figure 1 reveals an approximately sigmoidal relationship between the methyl chemical shift and concentration, implying the existence of two more or less discrete states, presumably monomer (favored in dilute solution) and an aggregate or a family of aggregates (favored in concentrated solution). Particularly noteworthy in Figure 1 is the large concentration range over which the transition from monomeric state to aggregated state occurs. The shallowness of this curve indicates that the aggregation of the disodium salt of **2** is only a very weakly cooperative phenomenon (i.e., the aggregation is noncritical).

The data in Figure 2 indicate that the aggregation of the disodium salt of **3g** is highly cooperative, because the monomer-to-aggregate transition occurs over a narrow concentration range. Further, aggregation of the disodium salt of **3g** occurs at substantially lower concentrations than the aggregation of the disodium salt of **2**. Aggregation of the disodium salt of **3g** can first be detected by ^{1}H NMR when the concentration approaches 2 mM and appears to be nearly complete (i.e., the ^{1}H chemical shift stops changing as a function of concentration) by 15 mM. Transitions that occur over such narrow concentration ranges are typical of micelle formation.[1] Analogous data sets for the disodium salts of the other diacids in the series **1–4** show that the transition from monomeric to aggregated states occurs over an increasingly narrow concentration range and at progressively lower concentrations as the length of the nonpolar tail increases (data are given in the supplementary material).

Data sets of the type shown in Figure 2 may be analyzed in a number of ways to determine a surfactant's critical micelle concentration (CMC).[1c,d] One common approach involves the application of the pseudo-phase-separation model, which treats the aggregate as a phase that separates from the solution containing the amphiphile.[16] Because the equilibrium between the monomeric and aggregated states is rapid on the ^{1}H NMR time scale, the chemical shift observed for an amphiphile proton at any concentration represents a weighted average of the chemical shifts for that proton in the monomeric and aggregated states. Monitored as a function of concentration, these chemical shifts vary smoothly between those of the fully solvated amphiphile and those of the amphiphile within the aggregate. For amphiphile concentrations above the CMC, applying the pseudo-phase-separation model to NMR chemical shift data gives eq 1

$$\delta_{obsd} = \delta_{agg} + CMC(\delta_{mon} - \delta_{agg})/C_{tot} \quad (1)$$

where C_{tot} is the total amphiphile concentration, δ_{obsd} is the observed chemical shift, and δ_{mon} and δ_{agg} are the chemical shifts of the amphiphile in the monomeric and aggregated states, respectively. According to the model, eq 2 holds for amphiphile concentrations below the CMC.

$$\delta_{obsd} = \delta_{mon} \quad (2)$$

The pseudo-phase-separation model therefore predicts that a plot of δ_{obsd} vs $1/C_{tot}$ should have two linear regions and the intersection of the lines should correspond to the CMC.[1c,16] Indeed, CMC values are often determined graphically from δ_{obsd} vs $1/C_{tot}$ plots in which only data points significantly below and significantly above the CMC are used to define the lines of interest.[1]

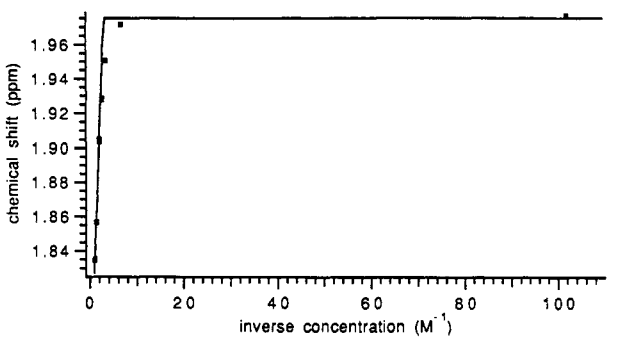

Figure 3. ^{1}H NMR chemical shift of the methyl group at C9 of the disodium salt of **2** as a function of the reciprocal of amphiphile concentration (30 °C). The smooth curve was generated by a fit to eqs 1 and 2, as described in the text. The derived CAC is 320 mM.

Analysis of data sets of the type shown in Figure 1 is somewhat more problematic, because the aggregation process is less cooperative (i.e., occurs over a wider concentration range) than is usually observed for micelle-forming processes. This behavior is not consistent with the pseudo-phase-separation model or more generally with the micelle hypothesis, both of which require that nearly all amphiphiles exist in the monomeric (unaggregated) state until concentrations very near the CMC are reached.[1] (Mukerjee et al. have observed similar noncritical behavior in the aggregation of bile salts,[4b] and noncritical aggregation has been observed for other amphiphile topologies as well.[2]) In order to compare aggregation behavior across the series **1–4**, we will use the term "critical aggregation concentration" (CAC) for all compounds we have studied, even though aggregation becomes less critical as molecular weight decreases.

Deviations from the idealized behavior postulated by the pseudo-phase-separation model are most apparent in the region of the CAC and at high concentrations.[16] Such deviations complicate the selection of the experimental points used to determine the CAC. In order to establish a method for CAC determination that is more systematic than selecting data points in linear regions of δ_{obsd} vs $1/C_{tot}$ plots by inspection and to assess the effect of nonideal deviations on the final CAC value for a given amphiphile, we fit entire ^{1}H NMR data sets to the step function shown in eq 3.

$$y = f_1(x)u_1 + f_2(x)u_2 \quad (3)$$

In eq 3, $u_1 = 1$ for concentrations less than the CAC, and $u_1 = 0$ for concentrations greater than the CAC; $u_2 = 0$ for concentrations less than the CAC, and $u_2 = 1$ for concentrations greater than the CAC. The functions $f_1(x)$ and $f_2(x)$ are defined in eqs 4 and 5.

$$f_1(x) = \delta_{agg} + CAC(\delta_{mon} - \delta_{agg})/C_{tot} \quad (4)$$

$$f_2(x) = \delta_{mon} \quad (5)$$

Figure 3 shows a δ_{obsd} vs $1/C_{tot}$ plot for the disodium salt of **2** along with the line generated for the best fit to eq 3 by simultaneous optimization of δ_{agg}, δ_{mon}, and CAC. Equation 3 was also used to generate the line shown in Figure 1 (same data set). Figure 4 shows a δ_{obsd} vs $1/C_{tot}$ plot for the disodium salt of **3g** along with the line generated for the best fit to eq 3, and the line in Figure 2 was also generated with eq 3.

In addition to determining the fit of a given data set in its entirety to eq 3, we also determined the fit of a constrained data set in which only concentration values below 3 times the CAC and 20% above or below the CAC were included. We found a substantial improvement in the fits of the constrained data set relative to the fits of the entire data sets to eq 3, but both the entire and constrained data sets generally provided similar CAC values

(16) Shinoda, K.; Hutchinson, E. *J. Phys. Chem.* **1962**, *66*, 577.

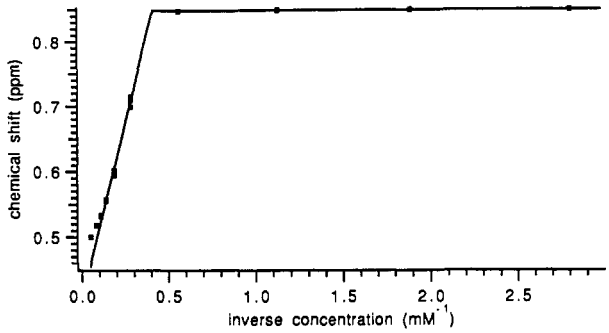

Figure 4. ^{1}H NMR chemical shift of the terminal methyl group on the alkyl chain of the disodium salt of **3g** as a function of the reciprocal of amphiphile concentration (30 °C). The smooth curve was generated by a fit to eqs 1 and 2, as described in the text. The derived CAC is 2.2 mM.

Table I. CAC Values Determined for Salts of Compounds **1–4**[a]

compd	fit to entire data set	fit to constrained set	dye solubilization
1[b]	510	500	
2[b]	350	380	
2	320	340	
3a	260	290	~390
3b	310	350	
3c	170	180	
3d	61	60	65
3e	17	18	
3e[c]	15	16	
3f	6.7	6.4	
3f[b]	6.3	6.3	
3g	2.2	2.4	3.0
3g[d]	3.6	3.7	
4	12	13	

[a] The values in the first two data columns were derived from ^{1}H NMR data, as described in the text. These values are based on the behavior of the lone methyl resonance in the spectra of **2–4**, unless otherwise indicated. Data obtained at 30 °C for disodium salts, unless otherwise indicated. [b] Values based on the behavior of an aromatic resonance. [c] Value based on the behavior of the dipotassium salt. [d] Value determined at 65 °C.

(within 5–10% of one another), as indicated by the data in Table I.

As mentioned above, the disodium salt of **3g** is not appreciably soluble in water at room temperature; however, the solubility of this salt is approximately 20 mM at 65 °C. When solutions of the disodium salt of **3g** were warmed gently to dissolve all solid and then cooled to 30 °C, the onset of precipitation was sufficiently slow that the ^{1}H NMR measurements required for CAC determination could be obtained at the lower temperature (the data shown in Figure 2 were obtained at 30 °C). In order to be certain that the CAC determined for the disodium salt of **3g** at 30 °C was not subject to artifacts resulting from supersaturation, the experiments summarized in Figure 2 were repeated at 65 °C. Analysis of the concentration dependence of the terminal methyl group ^{1}H NMR chemical shift leads to a CAC value of 3.6 mM at 65 °C (data given in the supplementary material), which is similar to the CAC value of 2.5 mM determined at 30 °C. The relatively small effect of this temperature variation on CMC is consistent with the behavior of many other micelle-forming surfactants.[1c] The similarity of the values determined for **3g** at 65 and 30 °C also indicates that the value determined at the lower temperature is not perturbed by supersaturation.

We used a dye solubilization method[17] to provide an independent measurement of the CAC values for **3a**, **3d**, and **3g** at room temperature. The dye orange OT is completely insoluble in aqueous solution but is solubilized by amphiphile aggregates. Therefore, determining the amount of dissolved dye (optical density at the dye λ_{max}) in a series of solutions containing varying amphiphile concentrations provides a data set that may be analyzed

(17) Schott, H. *J. Phys. Chem.* **1966**, *70*, 2966.

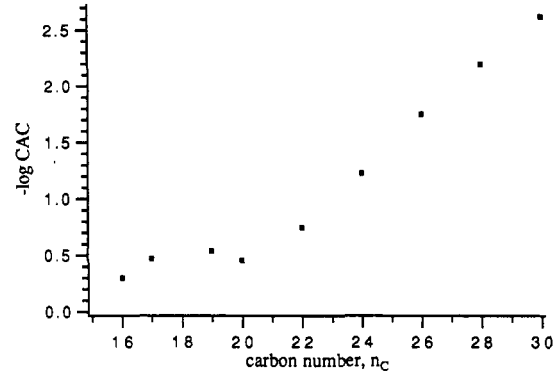

Figure 5. −log CAC as a function of carbon number (defined in text) for the disodium salts of **1**, **2**, and **3a–g**.

to provide a CAC value.[18] (Typically, a plot of dye absorbance vs amphiphile concentration is constructed; data points below the CAC fall on a line of approximately zero slope and intercept (no dye solubilized), and data above the CAC fall on a line with a positive slope. The intersection of these two lines defines the CAC.[17]) As indicated in Table I, the CAC values derived from the dye solubilization studies for **3a**, **3d**, and **3g** agree well with the values derived from NMR measurements. (The analyses may be found in the supplementary material.) Both NMR and dye solubilization data provide evidence of a gradual onset of aggregation of **3a**. The correlation of selected CAC values from two independent methods indicates that it is reasonable to rely on ^{1}H NMR data for characterization of aggregation behavior across the series **1–4**.

We were curious to know whether the sulfur atom in the tails of **3a–g**, introduced for synthetic efficiency, had any unusual effect on the aggregation behavior of **3a–g**. This issue is addressed by examining **4**, the analogue of **3e** in which the sulfur atom is replaced by a methylene group. ^{1}H NMR measurements indicated that the CAC for **4** was similar to, but slightly lower than, that for **3e** (13 vs 18 mM) and that the aggregation of the disodium salt of **4**, like the aggregation of the salt of **3e**, was highly cooperative (data given in the supplementary material). The similarity of CAC values for **3e** and **4** suggests that the sulfur atom of the former may be thought of as an approximate "methylene equivalent" in this context.[19]

Figure 5 shows a plot of −log CAC as a function of "carbon number" (n_c) for the disodium salts of **1–4**, where n_c is the total number of carbon atoms in each amphiphile, not including the carboxylate carbons. (The sulfur atoms in **3a–g** are counted as carbon atoms, which seems reasonable in light of the similar aggregation behavior of **3e** and **4**.) Linear relationships between log CMC and n_c have been previously observed for many families of surfactants (eq 6), and the slope of the correlation line (B) provided insight on the mode of aggregation.[1a] Figure 5 reveals

$$\log \mathrm{CMC} = A - B(n_c) \qquad (6)$$

that our amphiphiles fall into two groups with respect to aggregation properties: the aggregation of **1**, **2**, and **3a,b** is nonlinear and only weakly affected by changes in n_c, while the aggregation of **3c–g** shows a linear and more profound relationship to n_c. This analysis suggests that two distinct modes of aggregation are operative within this family of amphiphiles. Among the smaller molecules, the addition of nonpolar surface in the form of methylene groups and/or a sulfur atom has a relatively modest effect on the CAC. In the mode displayed by the molecules with longer tails, additional methylene groups exert a more substantial,

(18) One potential disadvantage of this technique is that the incorporation of nonpolar dye molecules might alter aggregate structure and stability. It is therefore possible that the CAC value for formation of mixed dye–amphiphile aggregates will be different from the CAC value for formation of pure amphiphile aggregates.

(19) A thioether sulfur atom and a methylene group are *not* functionally equivalent in at least some circumstances, see: Gellman, S. H. *Biochemistry* **1991**, *30*, 6633.

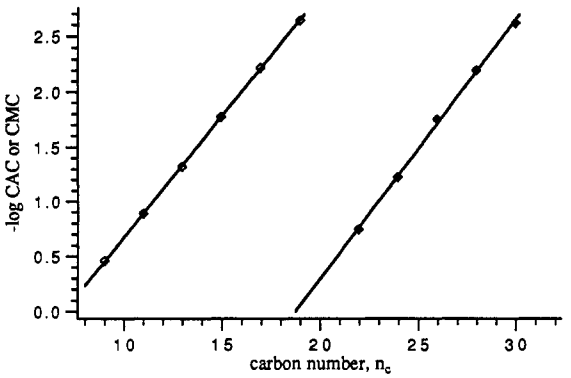

Figure 6. -log CAC as a function of carbon number (defined in text) for the disodium salts of **3c–g** (◆) and for the dipotassium salts of 2-octyl-, 2-decyl-, 2-dodecyl-, 2-tetradecyl-, 2-hexadecyl-, and 2-octadecylmalonate (◇; ref 20). The lines were obtained by linear regression. For **3c–g**, the slope is 0.24, and for the long chain alkylmalonates, the slope is 0.22.

enhancing effect on aggregation.

The cooperativity of aggregation among the disodium salts of **3d–g** and **4** and the relatively low CAC values measured for these amphiphiles suggest that these compounds undergo typical micellization processes. Among the family of amphiphiles discussed here, this mode of aggregation may be termed "tail-dominated". The lack of cooperativity and high CAC values among the disodium salts of **1**, **2**, and **3a,b** do not correspond to classical micelle-type behavior. This mode of aggregation may be designated "headgroup-dominated", because additional nonpolar units in the tail have less impact on the CAC values of these smaller amphiphiles than such additional nonpolar units do for the amphiphiles with longer tails. Our data provide little information on the structural differences between aggregates resulting from the headgroup-dominated and tail-dominated modes of association. Since the ^{1}H NMR resonances of all amphiphiles **1–4** remain reasonably narrow at concentrations well above the CAC, both types of aggregates must have a very dynamic structure, with individual amphiphiles rapidly sampling a variety of environments on the spectroscopic time scale.

Comparison with Other Types of Amphiphiles. Figure 6 shows a comparison of the log CMC vs n_c behavior reported for the dipotassium salts of long chain alkylmalonates[20] with our data for the disodium salts of **3c–g**. (The dipotassium salt of **3e** displays a CMC very similar to that of the disodium salt (data given in the supplementary material), 16 vs 18 mM, which suggests that it is reasonable to compare data for potassium and sodium salts.) The lines that best describe each amphiphile family (eq 6) have very similar slopes: for the malonate derivatives, $B = 0.22$,[21] and for **3c–g**, $B = 0.24$. However, the lines in Figure 6 are displaced from one another along the horizontal axis by $\Delta n_c = 11$. Since there are 16 carbon atoms, excluding the carboxylate carbons, in the rigid headgroup of **3c–g**, this horizontal displacement implies that the dibenzobarrelane headgroup promotes aggregation to an extent equivalent to only five methylene groups in a flexible nonpolar tail. Previous work has led to the conclusion that benzene rings embedded within a flexible hydrocarbon tail promote aggregation to an extent equivalent to about three and one-half methylene groups.[1a] The strikingly low "hydrophobic impact" of the rigid hydrocarbon headgroup of amphiphiles **3c–g** suggests that even the most effective micellar packing leaves a substantial portion of the headgroup's nonpolar surface exposed to solvent.

For a number of surfactant families possessing monoanionic headgroups and simple polymethylene tails, including the sodium and potassium salts of long chain carboxylates (fatty acids), B values of approximately 0.3 have been observed.[1a] The lower B value displayed by surfactants with relatively small dianionic headgroups, e.g., the long chain alkylmalonates ($B = 0.22$), may be qualitatively rationalized by invoking the greater interheadgroup electrostatic repulsion expected to occur for dianions relative to monoanions.[1] This additional repulsion should decrease the extent to which the nonpolar tails can associate closely with one another when attached to a malonate headgroup, with the result that each additional methylene group in the nonpolar chain exerts a smaller absolute effect in promoting aggregation of dianionic surfactants than in promoting aggregation of monoanionic surfactants. Our observations with **3c–g** provide indirect support for this explanation based on headgroup repulsion. We have already seen that, for the disodium salts of **3c–g**, B is identical to that of the alkylmalonates. For **3c–g**, one expects the nonpolar tails of neighboring amphiphiles to have difficulty in associating with one another not only because of electrostatic repulsion stemming from the double anionic charge but also because of steric repulsion between the aromatic rings projecting laterally from the headgroups.

Conclusion. The facile preparation of a homologous series of new amphiphiles has enabled us to examine the effects of an unusual amphiphilic topology on aggregation properties. The rigid dibenzobarrelanedicarboxylate unit itself (**1**) aggregates in a relatively noncooperative fashion, as do derivatives bearing short flexible nonpolar chains (**2** and **3a,b**). Derivatives bearing longer nonpolar chains (**3d–g**) undergo a more cooperative aggregation, which is typical of micelle formation. The effect of incremental increases in nonpolar chain length on the CAC values of these latter compounds indicates that the rigid headgroup makes a surprisingly modest contribution to the drive for aggregation. This deduction suggests that a substantial portion of the nonpolar surface of the headgroup may not be effectively sequestered from aqueous solution in the aggregate. Having characterized the basic aggregation behavior that stems from the attachment of a flexible lipophilic tail to a rigid headgroup of unusual topology, we are now in a position to examine the effects of the new amphiphiles on biomembranes and to explore the properties of more complex amphiphiles containing additional rigid units.

Experimental Section

Materials. Reagents were purchased from Aldrich Chemical Co. unless otherwise noted. THF and ether were distilled from benzophenone–sodium ketyl under N_2, and methylene chloride was distilled from calcium hydride under N_2. Low-conductivity D_2O for CAC studies was purchased from MSD Isotopes. Semiconductor-grade sodium and potassium hydroxides for diacid neutralization were purchased from Aldrich and Morton Thiokol, Inc., respectively. Aqueous NaOH and KOH solutions used for diacid neutralization were prepared with Millipore-filtered water and standardized with potassium hydrogen phthalate using phenolphthalein as an end point indicator. Orange OT was purified by water precipitation from acetone and two recrystallizations from ethanol.[17]

Instrumentation. NMR spectra were recorded on Bruker WP-200, WP-270, or AM-500 spectrometers. Proton chemical shifts were referenced relative to tetramethylsilane (TMS) and carbon shifts relative to $CDCl_3$. An external reference of sodium 3-(trimethylsilyl)-d_4-propionate (TSP) in D_2O was used for CAC studies. Routine NMR spectra were obtained in $CDCl_3$ at 200 MHz unless otherwise stated. Infrared spectra were obtained on a Mattson Polaris instrument. High-resolution electron-impact mass spectra (HRMS) were obtained on a Kratos MS-25 spectrometer. Fast atom bombardment (FAB) mass spectra were recorded at the University of Illinois. Melting points were determined on a Thomas-Hoover apparatus and were not corrected. In the descriptions of ^{1}H NMR data, we use the backbone numbering system shown for structure **10**.

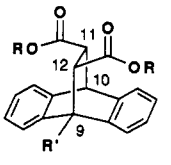

10

Synthetic Procedures. A. Thioethers (5a–g). Sodium metal was dissolved in degassed (N_2) absolute EtOH, 9-anthracenemethanethiol[22]

(20) (a) Shinoda, K. *J. Phys. Chem.* **1955**, *59*, 432. (b) Shinoda, K. *J. Phys. Chem.* **1956**, *60*, 1439. (c) See also: Vikingstad, E.; Saettersdal, H. *J. Colloid Interface Sci.* **1980**, *77*, 407.

(21) The original paper (ref 20a) reports a B value of 0.51 for the dipotassium salts of the long chain alkylmalonates, but it is clear from reanalysis of the data originally reported that this value is erroneous. Our reanalysis provides a B value of 0.22.

was added, and the resulting suspension was stirred for 1 h. Alkyl halide was added dropwise, and stirring was continued for 1 h. Additional EtOH was added if the suspension became too thick for stirring. Aqueous saturated NH_4Cl was then added, followed by water. The suspension was stirred for 30 min, and the suspended solid was isolated by vacuum filtration. Chromatography yielded the thioethers as yellow crystalline solids.

9-Anthracenylmethyl methyl sulfide (5a): 2.29 g, 9.62 mmol, 96%; mp 115.5–116.0 °C; IR (KBr pellet) 3048 (w), 2908 (2), 1622 (w), 1445 (m), 1239 (m), 744 (s) cm^{-1}; ^1H NMR δ 8.38 (br s, 1 H, ArH), 8.32 (m, 2 H, ArH), 7.99 (m, 2 H, ArH), 7.6–7.4 (m, 4 H, ArH), 4.71 (s, 2 H, $ArCH_2S$), 2.14 (s, 3 H, CH_3); HRMS calcd for $C_{16}H_{14}S$ (M^+) 238.0816, found 238.0815.

9-Anthracenylmethyl ethyl sulfide (5b): 5.36 g, 21.3 mmol, 97%; mp 69.5–70.5 °C; IR (KBr pellet) 2965 (w), 1443 (w), 1218 (w), 885 (m), 840 (w), 791 (w), 772 (s), 602 (w), 524 (m) cm^{-1}; ^1H NMR δ 8.39 (br s, 1 H, ArH), 8.34 (m, 2 H, ArH), 8.01 (m, 2 H, ArH), 7.60–7.43 (m, 4 H, ArH), 4.76 (s, 2 H, $ArCH_2S$), 2.70 (q, J = 7.4 Hz, 2 H, SCH_2CH_3), 1.36 (t, J = 7.4 Hz, 3 H, SCH_2CH_3); HRMS calcd for $C_{17}H_{16}S$ (M^+) 252.0973, found 252.0970.

9-Anthracenylmethyl butyl sulfide (5c): 3.46 g, 12.4 mmol, 95%; mp 50.0–51.0; IR (KBr pellet) 2960 (w), 1446 (w), 1217 (w), 888 (w), 842 (w), 727 (s) cm^{-1}; ^1H NMR δ 8.29 (br s, 1 H, ArH), 8.33 (m, 2 H, ArH), 8.00 (m, 2 H, ArH), 7.6–7.4 (m, 4 H, ArH), 4.74 (s, 2 H, $ArCH_2S$), 2.67 (t, J = 7.2 Hz, 2 H, SCH_2CH_2), 1.69 (m, 2 H, SCH_2CH_2), 1.44 (m, Hz, 2 H, CH_2CH_3), 0.91 (t, J = 7.3 Hz, 2 H, CH_3); HRMS calcd for $C_{19}H_{20}S$ (M^+) 280.1286, found 280.1276.

9-Anthracenylmethyl hexyl sulfide (5d): 2.16 g, 7.01 mmol, 79%; mp 45.0–48.0 °C; IR (KBr pellet) 2867 (w), 2855 (w), 1446 (w), 1411 (w), 890 (m), 843 (w), 792 (w), 732 (s) cm^{-1}; ^1H NMR δ 8.38 (br s, 1 H, ArH), 8.32 (m, 2 H, ArH), 7.99 (m, 2 H, ArH), 7.6–7.4 (m, 4 H, ArH), 4.70 (s, 2 H, $ArCH_2S$), 2.65 (t, J = 7.2 Hz, 2 H, SCH_2CH_2), 1.68 (m, 2 H, SCH_2CH_2), 1.5–1.2 (m, 6 H, chain CH_2's), 0.88 (t, J = 6.5, 3 H, CH_3); HRMS calcd for $C_{21}H_{24}S$ (M^+) 308.1599, found 308.1599.

9-Anthracenylmethyl octyl sulfide (5e): 5.61 g, 16.7 mmol, 76%; mp 43.5–44.0 °C; IR (KBr pellet) 2953 (w), 2922 (m), 2850 (w), 1470 (w), 876 (m), 722 (s) cm^{-1}; ^1H NMR δ 8.35 (br s, 1 H, ArH), 8.31 (m, 2 H, ArH), 7.97 (m, 2 H, ArH), 7.57–7.40 (m, 4 H, ArH), 4.70 (s, 2 H, $ArCH_2S$), 2.63 (t, J = 7.4 Hz, 2 H, SCH_2CH_2), 1.66 (m, 2 H, SCH_2CH_2), 1.5–1.2 (m, 10 H, chain CH_2's), 0.88 (t, J = 6.4 Hz, 3 H, CH_3); HRMS calcd for $C_{23}H_{28}S$ (M^+) 336.1912, found 336.1916.

9-Anthracenylmethyl decyl sulfide (5f): 1.36 g, 3.74 mmol, 94%; mp 44.0–45.0 °C; IR (KBr pellet) 2920 (s), 2850 (s), 1466 (m), 1445 (m), 881 (m), 733 (s), 723 (s) cm^{-1}; ^1H NMR δ 8.38 (br s, 1 H, ArH), 8.33 (m, 2 H, ArH), 8.00 (m, 2 H, ArH), 7.6–7.4 (m, 4 H, ArH), 4.73 (s, 2 H, $ArCH_2S$), 2.65 (t, J = 7.4 Hz, 2 H, SCH_2CH_2), 1.68 (m, 2 H, SCH_2CH_2), 1.5–1.2 (m, 14 H, chain CH_2's), 0.88 (t, J = 6.4 Hz, 3 H, CH_3); HRMS calcd for $C_{25}H_{32}S$ (M^+) 364.2225, found 364.2215.

9-Anthracenylmethyl dodecyl sulfide (5g): 690 mg, 1.76 mmol, 88%; mp 52.0–53.0 °C; IR (KBr pellet) 2934 (w), 2917 (w), 2851 (w), 1466 (w), 881 (m), 732 (s), 723 (s) cm^{-1}; ^1H NMR δ 8.39 (br s, 1 H, ArH), 8.33 (m, 2 H, ArH), 8.00 (m, 2 H, ArH), 7.59–7.42 (m, 4 H, ArH), 4.73 (s, 2 H, $ArCH_2S$), 2.66 (t, J = 7.4 Hz, 2 H, SCH_2CH_2), 1.68 (m, 2 H, SCH_2CH_2), 1.41–1.26 (m, 18 H, chain CH_2's), 0.88 (t, J = 6.4 Hz, 3 H, CH_3); HRMS calcd for $C_{27}H_{36}S$ (M^+) 392.2538, found 392.2528.

Nonyl 9-Anthryl Ketone (7). A solution of 9-acetylanthracene (3.0 g, 1.4 mmol) in 15 mL of benzene under N_2 was transferred via cannula into a suspension of NaH (411 mg, 17.1 mmol) in 15 mL of benzene under N_2, and the suspension was refluxed for 14 h. Octyl iodide (3.1 mL, 17 mmol) was added dropwise and refluxing continued for 4 days, over which time the gradual appearance of the product could be detected by TLC. The reaction was quenched with MeOH (3 mL), forming a clear, brown solution containing a white precipitate. The reaction mixture was passed through a short silica column with 100 mL of 10% EtOAc/hexanes. The solvent was evaporated to yield an orange solid that was further purified by chromatography (5% EtOAc/hexanes), affording the pure **7** (145 mg, 0.44 mmol, 3%) as a yellow solid and a larger portion of less pure material (2.0 g, 6.0 mmol, 43%) as a yellow oil: ^1H NMR δ 8.45 (s, 1 H, ArH), 8.00 (m, 2 H, ArH), 7.78 (m, 2 H, ArH), 7.53–7.42 (m, 4 H, ArH), 3.05 (t, J = 7.5 Hz, 2 H, $C(O)CH_2$), 1.88 (m, 2 H, $C(O)CH_2CH_2$), 1.41–1.26 (m, 12 H, chain CH_2's), 0.88 (t, J = 6.7 Hz, 3 H, CH_3).

1-(9-Anthryl)-1-decanol. To a solution of ketone **7** (2.0 g, 6.0 mmol) in 25 mL of toluene stirring under N_2 was added a mixture of toluene (12 mL) and 1 M $LiAlH_4$ in ether (12 mL, 1 M, 12 mmol) by cannula. The reaction was quenched after 30 min by the dropwise addition of freshly prepared saturated aqueous Na_2SO_4 solution until bubbling ceased. The cloudy yellow mixture was filtered through Celite, and the clear filtrate was concentrated to yield a residue that was purified by chromatography (5% EtOAc/hexanes) to afford 1-(9-anthryl)-1-decanol (862 mg, 2.58 mmol, 40%) as a red oil: ^1H NMR δ 8.64 (br s, 2 H, ArH), 8.36 (s, 1 H, ArH), 7.97 (m, 2 H, ArH), 7.51–7.39 (m, 4 H, ArH), 6.20 (m, 1 H, $CH(OH)CH_2$), 2.41, 2.13 (m, 2 H, $CH(OH)CH_2$), 1.62–1.22 (m, 14 H, chain CH_2's), 0.86 (t, J = 6.4 Hz, 3 H, CH_3).

1-(9-Anthryl)decane (8). Mesyl chloride (180 mL, 2.3 mmol) was added dropwise to a solution of 1-(9-anthryl)-1-decanol (662 mg, 2.0 mmol) and Et_3N (417 mL, 3.0 mmol) in CH_2Cl_2 (3 mL) that had been cooled to 0 °C in an ice–water bath. The solution was transferred after 30 min to a separatory funnel and extracted with 10 mL each of water, 1 M HCl, dilute aqueous $NaHCO_3$, brine, and water. The organic layer was then dried over anhydrous $MgSO_4$ and concentrated to yield the desired mesylate (530 mg, 1.3 mmol, 65%) as a yellow oil, which was used without further purification: ^1H NMR δ 8.90 (br d, J = 7.7 Hz, 1 H, ArH), 8.42 (s, 1 H, ArH), 8.25 (br d, J = 9.0 Hz, 1 H, ArH), 8.00 (br d, J = 8.3 Hz, 2 H, ArH), 7.57–7.45 (m, 4 H, ArH), 6.48 (t, J = 7.6 Hz, 1 H, $CH(OMs)CH_2$), 2.72, 2.53 (m, 2 H, $CH(OMs)CH_2$), 1.62–1.18 (m, 17 H, chain CH_2's, CH_3 (Ms)), 0.85 (t, J = 6.5 Hz, 3 H, CH_2CH_3).

To a solution of 488 mg (1.18 mmol) of this mesylate in 10 mL of toluene was added 2.4 mL (2.4 mmol) of a 1 M solution of $LiAlH_4$ in ether. After the reaction solution had been stirred for 15 min, a freshly prepared saturated aqueous Na_2SO_4 solution was added dropwise until bubbling ceased. The yellow reaction mixture was filtered through cotton to yield a clear, faintly yellow solution that was concentrated to afford **8** (369 mg, 1.16 mmol, 98%) as a light yellow oil containing crystalline solid, which was used without further purification: ^1H NMR δ 8.30 (br s, 1 H, ArH), 8.25 (m, 2 H, ArH), 7.99 (m, 2 H, ArH), 7.52–7.40 (m, 4 H, ArH), 3.58 (m, 2 H, $ArCH_2$), 1.80 (m, 2 H, $ArCH_2CH_2$), 1.70–1.20 (m, 14 H, chain CH_2's), 0.88 (t, J = 5.6 Hz, 3 H, CH_3); HRMS calcd for $C_{24}H_{30}$ (M^+) 318.2347, found 318.2334.

11,12-Dicarboxy-9,10-dihydro-9,10-ethanoanthracene dimethyl ester was prepared according to the procedure of Bachman and Scott,[12] in which anthracene and dimethyl fumarate are refluxed in *o*-xylene for 4 days. The crude product was purified by chromatography (10% EtOAc/hexanes) to yield the desired diester as an off-white crystalline solid in 67% yield: mp 106.5–107.0 °C (lit. mp 106–107 °C);[23] IR (KBr pellet) 2956 (w), 2950 (w), 1729 (s), 1722 (s), 1457 (m), 1430 (m), 1309 (m), 1266 (s), 1217 (s), 1195 (s), 1179 (s), 1167 (m), 1017 (s), 763 (m) cm^{-1}; ^1H NMR δ 7.35–7.05 (m, 8 H, ArH), 4.73 (br s, 2 H, H(9,10)), 3.63 (s, 6 H, CO_2CH_3), 3.42 (m, 2 H, H(11,12)); HRMS calcd for $C_{20}H_{18}O_4$ (M^+) 322.1205, found 322.1208.

9-Methyl-11,12-dicarboxy-9,10-dihydro-9,10-ethanoanthracene dimethyl ester was prepared in the same manner as the diester above (5.75 g, 17.1 mmol, 86%): mp 137.0–138.0 °C; IR (KBr pellet) 2967 (w), 2949 (w), 1735 (s), 1458 (s), 1437 (m), 1384 (m), 1330 (m), 1277 (s), 1231 (m), 1209 (s), 1177 (s), 1163 (s), 1138 (m), 1014 (m), 765 (m) cm^{-1}; ^1H NMR (270 MHz) δ 7.37–7.08 (m, 8 H, ArH), 4.72 (d, J = 2.4 Hz, H(12)), 3.62 (s, 3 H, CO_2CH_3), 3.60 (s, 3 H, CO_2CH_3), 3.22 (dd, J = 5.7, 2.4 Hz, 1 H, H(11)), 3.05 (d, J = 5.7 Hz, 1 H, H(10)), 1.98 (s, 3 H, $ArCH_3$); HRMS calcd for $C_{21}H_{20}O_4$ (M^+) 336.1362, found 336.1371.

B. Diesters (6a–g, 9). In a typical procedure, substituted anthracene **5a–g** or **8** was dissolved in freshly distilled CH_2Cl_2, and fumaryl chloride (1.1 equiv) was added. The resulting brown solution was stirred for 24–48 h, over which time the color became light yellow. Methanol (10 equiv) was then cautiously added dropwise and stirring continued for 1 h. Solvent was removed, and the yellow residue was chromatographed (10% EtOAc/hexanes) and then decolorized with activated carbon to yield a colorless, crystalline solid, generally in 50–95%.

9-[(Methylthio)methyl]-11,12-dicarboxy-9,10-dihydro-9,10-ethanoanthracene dimethyl ester (6a): mp 113.5–115.0 °C; IR (KBr pellet) 2910 (w), 2952 (w), 1739 (s), 1458 (m), 1432 (m), 1251 (m), 1223 (s), 1207 (s), 1194 (m), 1174 (m), 760 (m), 752 (m) cm^{-1}; ^1H NMR δ 7.64–7.06 (m, 8 H, ArH), 4.66 (d, J = 2.6 Hz, 1 H, H(12)), 3.79 (s, 2 H, CH_2 directly attached to ethanoanthracene), 3.64 (br s, 4 H, CO_2CH_3, H(10)), 3.57 (s, 3 H, CO_2CH_3), 3.14 (dd, J = 5.4, 2.7 Hz, 1 H, H(11)), 2.35 (s, 3 H, SCH_3); HRMS calcd for $C_{22}H_{22}OS$ (M^+) 382.1239, found 382.1246.

9-[(Ethylthio)methyl]-11,12-dicarboxy-9,10-dihydro-9,10-ethanoanthracene dimethyl ester (6b): mp 147.5–148.5 °C; IR (KBr pellet) 2960 (w), 2925 (w), 1743 (s), 1456 (m), 1436 (m), 1368 (m), 1212 (s), 1174 (s), 764 (m) cm^{-1}; ^1H NMR δ 7.64 (m, 1 H, ArH), 7.43 (m, 1 H, ArH), 7.33 (m, 1 H, ArH), 7.23–7.09 (m, 5 H, ArH), 4.65 (d, J = 2.6 Hz, 1 H, H(12)), 3.81 (s, 2 H, CH_2 directly attached to ethanoanthracene), 3.63 (s, 3 H, CO_2CH_3), ~3.6 (m, partially obscured, 1 H,

(22) Ciganek, E. *J. Org. Chem.* **1980**, *45*, 1497.

(23) Beilstein, 3rd Suppl., Vol. 9, pp 4660–4661.

H(10)), 3.56 (s, 3 H, CO_2CH_3), 3.12 (dd, J = 5.5, 2.7 Hz, 1 H, H(11)), 2.77 (q, J = 7.4, 2 H, SCH_2CH_2), 1.41 (t, J = 7.4 Hz, 3 H, CH_3); HRMS calcd for $C_{23}H_{24}O_4S$ (M^+) 396.1395, found 396.1411.

9-[(Butylthio)methyl]-11,12-dicarboxy-9,10-dihydro-9,10-ethanoanthracene dimethyl ester (6c): mp 80.5–82.5 °C; IR (KBr pellet) 2957 (m), 2918 (m), 2847 (w), 1745 (s), 1737 (s), 1457 (m), 1437 (m), 1215 (s), 1174 (s), 761 (m), 750 (m) cm^{-1}; ^1H NMR δ 7.7–7.1 (m, 8 H, ArH), 4.64 (d, J = 2.2 Hz, 1 H, H(12)), 3.80 (s, 2 H, CH_2 directly attached to ethanoanthracene), 3.64 (s, 3 H, CO_2CH_3), ~3.6 (m, partially obscured, 1 H, H(10)), 3.56 (s, 3 H, CO_2CH_3), 3.11 (dd, J = 5.1, 2.4 Hz, 1 H, H(11)), 2.75 (t, J = 7.2, 2 H, SCH_2CH_2), 1.73 (m, 2 H, SCH_2CH_2), 1.52 (m, 2 H, CH_2CH_3), 0.98 (t, J = 7.3 Hz, 3 H, CH_2CH_3); HRMS calcd for $C_{25}H_{28}O_4S$ (M^+) 424.1708, found 424.1701.

9-[(Hexylthio)methyl]-11,12-dicarboxy-9,10-dihydro-9,10-ethanoanthracene dimethyl ester (6d): mp 73.0–75.0 °C; IR (KBr pellet) 2854 (m), 2847 (m), 1737 (s), 1457 (s), 1431 (s), 1221 (s), 1205 (s), 1195 (s), 757 (s) cm^{-1}; ^1H NMR δ 7.64 (m, 1 H, ArH), 7.44–7.08 (m, 7 H, ArH), 4.64 (d, J = 2.7 Hz, 1 H, H(12)), 3.80 (s, 2 H, CH_2 directly attached to ethanoanthracene), 3.63 (s, 3 H, CO_2CH_3), ~3.6 (m, partially obscured, 1 H, H(10)), 3.55 (s, 3 H, CO_2CH_3), 3.11 (dd, J = 5.5, 2.7 Hz, 1 H, H(11)), 2.73 (t, J = 7.4, 2 H, SCH_2CH_2), 1.74 (m, 2 H, SCH_2CH_2), 1.51–1.28 (m, 6 H, chain CH_2's), 0.92 (t, J = 6.6 Hz, 3 H, CH_2CH_3); HRMS calcd for $C_{27}H_{32}O_4S$ (M^+) 452.2021, found 452.1999.

9-[(Octylthio)methyl]-11,12-dicarboxy-9,10-dihydro-9,10-ethanoanthracene dimethyl ester (6e) (6.99 g) was isolated as a colorless oil containing trapped solvent. Only a portion of this material was purified, and an analytical sample gave the following spectral results: mp 73.0–75.0 °C; IR (KBr pellet) 2925 (m), 2853 (m), 1730 (s), 1458 (m), 1432 (m), 1222 (s), 1173 (m), 758 (m) cm^{-1}; ^1H NMR δ 7.64 (m, 1 H, ArH), 7.44–7.09 (m, 7 H, ArH), 4.64 (d, J = 2.6 Hz, 1 H, H(12)), 3.80 (s, 2 H, CH_2 directly attached to ethanoanthracene), 3.64 (s, 3 H, CO_2CH_3), ~3.6 (m, partially obscured, 1 H, H(10)), 3.56 (s, 3 H, CO_2CH_3), 3.11 (dd, J = 5.5, 2.7 Hz, 1 H, H(11)), 2.74 (t, J = 7.4, 2 H, SCH_2CH_2), 1.74 (m, 2 H, SCH_2CH_2), 1.52–1.31 (m, 10 H, chain CH_2's), 0.90 (t, J = 6.7 Hz, 3 H, CH_2CH_3); HRMS calcd for $C_{29}H_{36}O_4S$ (M^+) 480.2334, found 480.2323.

9-[(Decylthio)methyl]-11,12-dicarboxy-9,10-dihydro-9,10-ethanoanthracene dimethyl ester (6f): mp 69.5–71.0 °C; IR (KBr pellet) 2925 (m), 2853 (m), 1731 (s), 1458 (m), 1432 (m), 1222 (s), 1204 (s), 758 (s) cm^{-1}; ^1H NMR δ 7.64 (m, 1 H, ArH), 7.43 (m, 1 H, ArH), 7.33 (m, 1 H, ArH), 7.24–7.09 (m, 5 H, ArH), 4.64 (d, J = 2.6 Hz, 1 H, H(12)), 3.80 (s, 2 H, CH_2 directly attached to ethanoanthracene), 3.64 (s, 3 H, CO_2CH_3), ~3.63 (m, partially obscured, 1 H, H(10)), 3.56 (s, 3 H, CO_2CH_3), 3.11 (dd, J = 5.5, 2.6 Hz, 1 H, H(11)), 2.74 (t, J = 7.2, 2 H, SCH_2CH_2), 1.74 (m, 2 H, SCH_2CH_2), 1.5–1.29 (m, 14 H, chain CH_2's), 0.89 (t, J = 6.5 Hz, 3 H, CH_2CH_3); HRMS calcd for $C_{31}H_{40}O_4S$ (M^+) 508.2647, found 508.2649.

9-[(Dodecylthio)methyl]-11,12-dicarboxy-9,10-dihydro-9,10-ethanoanthracene dimethyl ester (6g): mp 55.5–67.0 °C; IR (KBr pellet) 2853 (w), 1742 (s), 1457 (m), 1437 (m), 1218 (s), 1178 (s), 758 (s) cm^{-1}; ^1H NMR δ 7.64 (m, 1 H, ArH), 7.43 (m, 1 H, ArH), 7.33 (m, 1 H, ArH), 7.23–7.09 (m 5 H, ArH), 4.64 (d, J = 2.6 Hz, 1 H, H(12)), 3.80 (s, 2 H, CH_2 directly attached to ethanoanthracene), 3.64 (s, 3 H, CO_2CH_3), ~3.63 (m, partially obscured, 1 H, H(10)), 3.56 (s, 3 H, CO_2CH_3), 3.11 (dd, J = 5.5, 2.7 Hz, 1 H, H(11)), 2.73 (t, J = 7.3 Hz, 2 H, SCH_2CH_2), 1.74 (m, 2 H, SCH_2CH_2), 1.46–1.28 (m, 18 H, chain CH_2's), 0.88 (t, J = 6.4 Hz, 3 H, CH_2CH_3); HRMS calcd for $C_{33}H_{44}O_4S$ (M^+) 536.2960, found 536.2943.

9-Decyl-11,12-dicarboxy-9,10-dihydro-9,10-ethanoanthracene dimethyl ester (9): mp 66.0–67.0 °C; IR (KBr pellet) 2923 (m), 2851 (m), 1745 (s), 1468 (m), 1459 (m), 1435 (m), 1214 (s), 1203 (s), 1175 (s), 756 (s) cm^{-1}; ^1H NMR δ 7.33–7.06 (m, 8 H, ArH), 4.65 (d, J = 2.6 Hz, 1 H, H(12)), 3.64 (s, 3 H, CO_2CH_3), 3.55 (s, 3 H, CO_2CH_3), 3.34 (d, J = 5.3 Hz, 1 H, H(10)), 3.17 (dd, J = 5.3, 2.6 Hz, 1 H, H(11)), 2.46 (m, 2 H, CH_2 directly attached to ethanoanthracene), 1.89 (m, 2 H, H(16)), 1.70–1.25 (m, 14 H, chain CH_2's), 0.90 (t, J = 7.0 Hz, 3 H, CH_2CH_3); HRMS calcd for $C_{30}H_{38}O_4$ (M^+) 462.2770, found 462.2775.

C. Diacids (1, 2, 3a–g, 4). In a typical reaction, aqueous sodium hydroxide was added to a solution of the diester (**6a–g, 9**) in MeOH, forming a white suspension that was refluxed until clear. The cooled solution was diluted with water, and the diacid was precipitated with concentrated HCl. The precipitated diacid was isolated either by filtration or by extraction with $CHCl_3$; in the latter situation, the combined extracts were dried over anhydrous $MgSO_4$ and evaporated to yield a clear oil, which was triturated with ether to initiate solidification. Diacids were dried at 100 °C under vacuum over P_2O_5 for 1–2 days.

11,12-Dicarboxy-9,10-dihydro-9,10-ethanoanthracene (1): 2.52 g, 8.57 mmol, 66%; mp 248.0–251.0 °C dec (lit. mp 241–243 °C);[23] ^1H NMR (DMSO, 200 MHz) δ 7.39 (m, 2 H, ArH), 7.25 (m, 2 H, ArH), 7.08 (m, 4 H, ArH), 4.71 (s, 2 H, H(9,12)), 3.11 (s, 2 H, H(10,11)); HRMS calcd for $C_{18}H_{14}O_4$ (M^+) 294.0892, found 294.0895.

9-Methyl-11,12-dicarboxy-9,10-dihydro-9,10-ethanoanthracene (2): 2.13 g, 6.92 mmol, 58%; mp 225.0–226.5 °C dec; ^1H NMR (DMSO-d_6, 200 MHz) δ 7.40–7.05 (m, 8 H, ArH), 4.69 (d, J = 2.2 Hz, 1 H, H(12)), 2.99 (dd, J = 5.9, 2.4 Hz, 1 H, H(11)), 2.74 (d, J = 5.9 Hz, 1 H, H(10)), 1.94 (s, 3 H, CH_3); HRMS calcd for $C_{19}H_{16}O_4$ (M^+) 308.1049, found 308.1046.

9-[(Methylthio)methyl]-11,12-dicarboxy-9,10-dihydro-9,10-ethanoanthracene (3a): 1.51 g, 4.27 mmol, 81%; mp 171.0–173.0 °C dec; ^1H NMR (DMSO-d_6, 200 MHz) δ 7.52–7.04 (m, 8 H, ArH), 4.64 (d, J = 2.4 Hz, 1 H, H(12)), 3.81 (AB q, J_{AB} = 12.6 Hz, $\Delta\nu$ = 14.3 Hz, 2 H, CH_2 directly attached to ethanoanthracene), ~3.3 (1 H, H(10)), 2.92 (dd, J = 5.6, 2.5 Hz, 1 H, H(11)), 2.31 (s, 3 H, CH_3); HRMS calcd for $C_{20}H_{18}O_4S$ (M^+) 354.0926, found 354.0939.

9-[(Ethylthio)methyl]-11,12-dicarboxy-9,10-dihydro-9,10-ethanoanthracene (3b): 1.10 g, 2.99 mmol, 73%; mp 171.0–173.0 °C dec; ^1H NMR (DMSO-d_6, 200 MHz) δ 7.53–7.03 (m, 7 H, ArH), 4.65 (d, J = 2.5 Hz, 1 H, H(12)), 3.82 (br s, 2 H, CH_2 directly attached to ethanoanthracene), 3.53 (br d, J = 4.8 Hz, 1 H, H(10)), 3.22 (dd, J = 5.7, 2.5 Hz, 1 H, H(11)), 2.75 (t, J = 7.0 Hz, 2 H, SCH_2CH_2), 1.75 (m, 2 H, SCH_2CH_2), 1.46–1.32 (m, 10 H, chain CH_2's), 0.90 (t, J = 6.7 Hz, 3 H, CH_3); FAB MS 369 (MH^+).

9-[(Butylthio)methyl]-11,12-dicarboxy-9,10-dihydro-9,10-ethanoanthracene (3c): 1.07 g, 2.70 mmol, 82%; mp 169.0–173.0 °C dec; ^1H NMR (DMSO-d_6, 200 MHz) δ 7.54–7.03 (m, 8 H, ArH), 4.64 (d, J = 2.5 Hz, 1 H, H(12)), 3.84 (AB q, J = 12.4 Hz, $\Delta\nu$ = 28.8 Hz, 2 H, CH_2 directly attached to ethanoanthracene), 3.35 (d, J = 5.0 Hz, 1 H, H(10)), 2.91 (dd, J = 5.7, 2.6 Hz, 1 H, H(11)), 2.74 (t, J = 7.1 Hz, 2 H, SCH_2CH_2), 1.68 (m, 2 H, SCH_2CH_2), 1.45 (m, 2 H, CH_2CH_3), 0.94 (t, J = 7.3 Hz, 3 H, CH_3); FAB MS 397 (MH^+).

9-[(Hexylthio)methyl]-11,12-dicarboxy-9,10-dihydro-9,10-ethanoanthracene (3d): 1.24 g, 2.92 mmol, 40%; mp 193.5–194.5 °C dec; ^1H NMR δ 7.7–7.1 (m, 8 H, ArH), 4.64 (d, J = 2.5 Hz, 1 H, H(12)), 3.81 (m, 2 H, CH_2 directly attached to ethanoanthracene), 3.54 (br d, J = 5 Hz, 1 H, H(10)), 3.22 (dd, J = 5.6, 2.6 Hz, 1 H, H(11)), 2.75 (t, J = 7.0 Hz, 2 H, SCH_2CH_2), 1.74 (m, 2 H, SCH_2CH_2), 1.5–1.2 (m, 6 H, chain CH_2's), 0.93 (t, J = 6.5 Hz, 3 H, CH_3); HRMS calcd for $C_{25}H_{28}O_4S$ (M^+) 424.1708, found 424.1709.

9-[(Octylthio)methyl]-11,12-dicarboxy-9,10-dihydro-9,10-ethanoanthracene (3e): 4.70 g, 10.4 mmol, 87%; mp 173.0–174.5 °C; ^1H NMR δ 7.64 (m, 1 H, ArH), 7.37–7.06 (m, 7 H, ArH), 4.65 (d, J = 2.5 JHz, 1 H, H(12)), 3.82 (br s, 2 H, CH_2 directly attached to ethanoanthracene), 3.53 (br d, J = 4.8 Hz, 1 H, H(10)), 3.22 (dd, J = 5.7, 2.5 Hz, 1 H, H(11)), 2.75 (t, J = 7.0, 2 H, SCH_2CH_2), 1.75 (m, 2 H, SCH_2CH_2), 1.46–1.32 (m, 10 H, chain CH_2's), 0.90 (t, J = 6.7 Hz, 3 H, CH_3); HRMS calcd for $C_{27}H_{32}O_4S$ (M^+) 452.2021, found 452.1996.

9-[(Decylthio)methyl]-11,12-dicarboxy-9,10-dihydro-9,10-ethanoanthracene (3f): 1.2 g, 2.5 mmol, quant.; mp 149.5–153.5 °C dec; ^1H NMR δ 7.64 (m, 1 H, ArH), 7.34–7.10 (m, 7 H, ArH), 4.66 (d, J = 2.4 Hz, 1 H, H(12)), 3.82 (br s, 2 H, CH_2 directly attached to ethanoanthracene), 3.54 (br d, J = 5 Hz, 1 H, H(10)), 3.22 (dd, J = 5.6, 2.5 Hz, 1 H, H(11)), 2.75 (t, J = 7.2 Hz, 2 H, SCH_2CH_2), 1.75 (m, 2 H, SCH_2CH_2), 1.46–1.24 (m, 14 H, chain CH_2's), 0.90 (t, J = 6.7 Hz, 3 H, CH_3); FAB MS 481 (MH^+).

9-[(Dodecylthio)methyl]-11,12-dicarboxy-9,10-dihydro-9,10-ethanoanthracene (3g): 342 mg, 0.67 mmol, 98%; mp 95.5–98.0 °C dec; ^1H NMR δ 7.65 (m, 1 H, ArH), 7.37–7.07 (m, 7 H, ArH), 4.67 (d, J = 2.4 Hz, 1 H, H(12)), 3.82 (m, 2 H, CH_2 directly attached to ethanoanthracene), 3.53 (br d, J = 5.8 Hz, 1 H, H(10)), 3.25 (dd, J = 5.7, 2.6 Hz, 1 H, H(11)), 2.76 (t, J = 6.8 Hz, 2 H, SCH_2CH_2), 1.75 (m, 2 H, SCH_2CH_2), 1.52–1.28 (m, 18 H, chain CH_2's), 0.88 (t, J = 6.9 Hz, 3 H, CH_3); FAB MS 509 (MH^+).

9-Decyl-11,12-dicarboxy-9,10-dihydro-9,10-ethanoanthracene (4): 182 mg, 0.42 mmol, 72%; mp 151.0–154.5 °C dec; ^1H NMR (DMSO-d_6, 200 MHz) δ 7.36–7.02 (m, 8 H, ArH), 4.63 (d, J = 2.5 Hz, 1 H, H(12)), 3.05 (d, J = 5.4 Hz, 1 H, H(10)), 2.96 (dd, J = 5.4, 2.4 Hz, 1 H, H(11)), 2.6–2.3 (m, 2 H, CH_2 directly attached to ethanoanthracene), 1.80 (m, 2 H, H(16)), 1.59–1.27 (m, 14 H, chain CH_2's), 0.86 (t, J = 6.8 Hz, 3 H, CH_3); HRMS calcd for $C_{28}H_{34}O_4$ (M^+) 434.2457, found 434.2437.

D. Diacid Salts. Diacids were neutralized with a 2–5 mol % excess of standardized base to avoid interference by carbon dioxide. The clear solutions were lyophilized and further dried at 100 °C under vacuum over P_2O_5 for 1–2 days, yielding fluffy white solids.

11,12-Dicarboxy-9,10-dihydro-9,10-ethanoanthracene disodium salt: IR (KBr pellet) 3400 (br, s), 1568 (s), 1465 (w), 1457 (w), 1410 (s) cm^{-1}; ^1H NMR (D_2O, 500 MHz, 45 mM) δ 7.45–7.14 (m, 8 H, ArH), 4.69 (s, 2 H, H(9,12)), 3.09 (s, 2 H, H(11,12)).

9-Methyl-11,12-dicarboxy-9,10-dihydro-9,10-ethanoanthracene disodium salt: IR (KBr pellet) 3400 (br, s), 1576 (s), 1563 (s), 1456 (m), 1393 (s), 1390 (s), 1306 (w) cm^{-1}; ^1H NMR (D_2O, 500 MHz, 51 mM)

δ 7.44–7.14 (m, 8 H, ArH), 4.63 (d, J = 2.1 Hz, 1 H, H(12)), 2.87 (dd, J = 6.2, 2.2 Hz, 1 H, H(11)), 2.73 (d, J = 6.2 Hz, 1 H, H(10)), 1.98 (s, 3 H, CH_3).

9-[(Methylthio)methyl]-11,12-dicarboxy-9,10-dihydro-9,10-ethanoanthracene disodium salt: IR (KBr pellet) 3400 (br, s), 1582 (s), 1575 (s), 1563 (s), 1467 (m), 1456 (m), 1407 (s), 1389 (s), 1322 (m), 1310 (m) cm^{-1}; ^1H NMR (D_2O, 500 MHz, 72 mM) δ 7.63–7.16 (m, 8 H, ArH), 4.59 (d, J = 2.2 Hz, 1 H, H(12)), 3.78 (AB q, J = 12.8 Hz, $\Delta\nu$ = 11 Hz, 2 H, CH_2 directly attached to ethanoanthracene), 2.99 (br s, 1 H, H(10)), 2.76 (dd, J = 6.0, 2.3 Hz, 1 H, H(11)), 2.41 (s, 3 H, CH_3).

9-[(Ethylthio)methyl]-11,12-dicarboxy-9,10-dihydro-9,10-ethanoanthracene disodium salt: IR (KBr) 3200 (br, s), 1654 (m), 1578 (s), 1573 (s), 1563 (s), 1547 (s), 1408 (s), 1400 (s), 1380 (s) cm^{-1}; ^1H NMR (D_2O, 500 MHz, 140 mM) δ 7.64 (m, 1 H, ArH), 7.52 (m, 1 H, ArH), 7.43 (m, 1 H, ArH), 7.32 (m, 1 H, ArH), 7.24–7.16 (m, 4 H, ArH), 4.59 (d, J = 2.2 Hz, 1 H, H(12)), 3.79 (AB q, J_{AB} = 12.7 Hz, $\Delta\nu$ = 24.0 Hz, 2 H, CH_2 directly attached to ethanoanthracene), 2.98 (br s, 1 H, H-(10)), 2.87 (q, J = 7.4 Hz, 2 H, SCH_2CH_2), 2.76 (dd, J = 6.0, 2.3 Hz, 1 H, H(11)), 1.41 (t, J = 7.4 Hz, 3 H, CH_3); FAB MS 413 (MH^+).

9-[(Butylthio)methyl]-11,12-dicarboxy-9,10-dihydro-9,10-ethanoanthracene disodium salt: IR (KBr pellet) 3500 (br), 2850 (m), 1576 (s), 1390 (s) cm^{-1}; ^1H NMR (D_2O, 200 MHz, 22 mM) δ 7.66 (m, 1 H, ArH), 7.53 (m, 1 H, ArH), 7.44 (m, 1 H, ArH), 7.33 (m, 1 H, ArH), 7.24–7.17 (m, 4 H, ArH), 4.60 (d, J = 2.2 Hz, 1 H, H(12)), 3.78 (AB q, J_{AB} = 12.7 Hz, $\Delta\nu$ = 28.2 Hz, 2 H, CH_2 directly attached to ethanoanthracene), ~2.95 (m, partially obscured, 1 H, H(10)), 2.90 (t, J = 7.3 Hz, 2 H, CH_2CH_2), 2.76 (dd, J = 6.0, 2.3 Hz, 1 H, H(11)), 1.78 (m, SCH_2CH_2), 1.53 (m, 2 H, CH_2CH_3), 0.98 (t, J = 7.4 Hz, 3 H, CH_3).

9-[(Hexylthio)methyl]-11,12-dicarboxy-9,10-dihydro-9,10-ethanoanthracene disodium salt: IR (KBr pellet) 3400 (br s), 2897 (m), 1597 (s), 1577 (s), 1571 (s), 1564 (s), 1457 (m), 1406 (s), 1397 (s), 1390 (s) cm^{-1}; ^1H NMR (D_2O, 500 MHz, 24 mM) δ 7.66 (m, 1 H, ArH), 7.53 (m, 1 H, ArH), 7.45 (m, 1 H, ArH), 7.33 (m, 1 H, ArH), 7.25–7.16 (m, 4 H, ArH), 4.60 (d, J = 2.2 Hz, 1 H, H(12)), 3.77 (AB q, J_{AB} = 12.7 Hz, $\Delta\nu$ = 34.0 Hz, 2 H, CH_2 directly attached to ethanoanthracene), 2.93 (br s, 1 H, H(10)), 2.89 (t, J = 7.3 Hz, 2 H, SCH_2CH_2), 2.76 (dd, J = 6.0, 2.3 Hz, 1 H, H(11)), 1.78 (m, 2 H, SCH_2CH_2), 1.50 (m, 2 H, CH_2CH_3), 1.41–1.34 (m, 4 H, chain CH_2's), 0.92 (t, J = 7.1 Hz, 3 H, CH_3).

9-[(Octylthio)methyl]-11,12-dicarboxy-9,10-dihydro-9,10-ethanoanthracene disodium salt: IR (KBr pellet) 3400 (br, s), 2921 (m), 2847 (w), 1572 (s), 1563 (s), 1558 (s), 1549 (s), 1454 (s), 1445 (s), 1410 (s), 1389 (s) cm^{-1}; ^1H NMR (D_2O, 500 MHz, 17 mM) δ 7.65 (m, 1 H, ArH), 7.52 (m, 1 H, ArH), 7.43 (m, 1 H, ArH), 7.32 (m, 1 H, ArH), 7.23–7.15 (m, 4 H, ArH), 4.59 (d, J = 2.1 Hz, 1 H, H(12)), 3.76 (AB q, J_{AB} = 12.6 Hz, $\Delta\nu$ = 42.3 Hz, 2 H, CH_2 directly attached to ethanoanthracene), 2.93 (br s, 1 H, H(10)), 2.83 (t, J = 7.2 Hz, 2 H, SCH_2CH_2), 2.75 (dd, J = 6.0, 2.3 Hz, 1 H, H(11)), 1.73 (m, 2 H, SCH_2CH_2), 1.45 (m, 2 H, $SCH_2CH_2CH_2$), 1.27 (m, 8 H, chain CH_2's), 0.85 (t, J = 6.9 Hz, 3 H, CH_3); FAB MS 497 (MH^+).

9-[(Decylthio)methyl]-11,12-dicarboxy-9,10-dihydro-9,10-ethanoanthracene disodium salt: IR (KBr pellet) 3500 (br, m), 2918 (m), 1574 (s), 1562 (s), 1557 (s), 1469 (w), 1457 (w), 1409 (m), 1404 (m), 1385 (m) cm^{-1}; ^1H NMR (D_2O, 500 MHz, 2.4 mM) δ 7.62 (m, 1 H, ArH), 7.48 (m, 1 H, ArH), 7.38 (m, 1 H, ArH), 7.28 (m, 1 H, ArH), 7.20–6.99 (m, 4 H, ArH), 4.55 (d, J = 2.0 Hz, 1 H, H(12)), 3.72 (m, 2 H, CH_2 directly attached to ethanoanthracene), ~2.90 (m, partially obscured, 1 H, H(10)), 2.85 (t, J = 7.2 Hz, 2 H, SCH_2CH_2), 2.71 (dd, J = 5.9, 2.3 Hz, 1 H, H(11)), 1.75 (m, 2 H, SCH_2CH_2), 1.46–1.24 (m, 14 H, chain CH_2's), 0.82 (t, J = 7.2 Hz, 3 H, CH_3).

9-[(Dodecylthio)methyl]-11,12-dicarboxy-9,10-dihydro-9,10-ethanoanthracene disodium salt: IR (KBr pellet) 3500 (br, m), 2895 (m), 1575 (s), 1563 (s), 1456 (m), 1410 (s), 1384 (s) cm^{-1}; ^1H NMR (D_2O, 500 MHz, 1.8 mM), δ 7.67 (m, 1 H, ArH), 7.54 (m, 1 H, ArH), 7.44 (m, 1 H, ArH), 7.33 (m, 1 H, ArH), 7.24–7.18 (m, 4 H, ArH), 4.59 (d, J = 2.1 Hz, 1 H, H(12)), 3.78 (AB q, J_{AB} = 12.6 Hz, $\Delta\nu$ = 33.2 Hz, 2 H, CH_2 directly attached to ethanoanthracene), ~2.92 (br s, 1 H, H-(10)), 2.91 (t, J = 6.8 Hz, 2 H, SCH_2CH_2), 2.76 (dd, J = 6.0, 2.1 Hz, 1 H, H(11)), 1.80 (m, 2 H, SCH_2CH_2), 1.52 (m, 2 H, $SCH_2CH_2CH_2$), 1.34–1.26 (m, 16 H, chain CH_2's), 0.85 (t, J = 5.9 Hz, 3 H, CH_3); FAB MS 553 (MH^+).

9-Decyl-11,12-dicarboxy-9,10-dihydro-9,10-ethanoanthracene disodium salt: IR (KBr pellet) 3500 (br, w), 2910 (m), 2853 (w), 1598 (m), 1577 (s), 1571 (s), 1560 (s), 1551 (s), 1457 (w), 1410 (m), 1385 (m) cm^{-1}; ^1H NMR (D_2O, 500 MHz, 9.3 mM) δ 7.40–7.13 (m, 8 H, ArH), 4.55 (d, J = 2.3 Hz, 1 H, H(12)), 2.92 (d, J = 6.3 Hz, 1 H, H(10)), 2.74 (dd, J = 6.2, 2.3 Hz, 1 H, H(11)), 2.53–2.40 (m, 2 H, CH_2 directly attached to ethanoanthracene), 1.90 (m, 2 H, H(16)), 1.65–1.32 (m, 14 H, chain CH_2's), 0.89 (t, J = 7.0 Hz, 3 H, CH_3).

CAC Determination: ^1H NMR. A 2-mL stock solution of the diacid salt at a concentration 3–4 times greater than the CAC was diluted to provide NMR samples at concentrations above the below the CAC. Proton spectra were recorded at a constant temperature (30 or 65 °C) on an AM-500 spectrometer.

CAC Determination: Dye Solubilization. A 5- or 10-mL stock solution of the diacid salt at a concentration 3 times greater than the CAC was diluted to provide 1- or 2-mL samples at series of concentrations above and below the CAC. Sufficient solid orange OT was added to saturate each sample. Teflon-lined screw-capped tubes containing the samples were gently rocked at room temperature for 1–3 days. Samples were filtered through cotton, 200-μL aliquots were diluted with 800 μL of absolute ethanol, and absorbance was measured at 500 nm.

Curve Fitting. Chemical shift vs inverse concentration data were iteratively fit to a user-defined function using Igor 1.24 (Wave Metrics, Lake Oswego, OR). Our user-defined function, ((w[1]+((1/w[0])*(w-[2]-w[1])*xx))*log(sign(w[0]-xx)+2)/log(3)+w[2]*log(sign(xx-w-[0])+2)/log(3)) (in the terminology required by Igor), mimics a step function by using Igor's sign feature to force one term or the other to equal zero in appropriate concentration ranges, as required by the pseudo-phase-separation model (eqs 1 and 2).

Krafft Point Determination. Solutions containing suspended amphiphile in 5-mm diameter NMR sample tubes were cooled to 4 °C and warmed gently in a heated water bath with agitation. The temperature was gradually increased until all solid dissolved.

Acknowledgment. This work was supported by the National Institutes of Health (GM-41825) and, in the initial phases, by Cambridge NeuroScience Research, Inc. T.M.S. thanks the Graduate School of the University of Wisconsin—Madison for a research assistantship, and S.H.G. is grateful for support from the Searle Scholars Program, the American Cancer Society (Junior Faculty Research Award), the National Science Foundation (Presidential Young Investigator Program), and the Eastman Kodak Company. We thank Professor P. Mukerjee for helpful discussions.

Registry No. 1, 36326-57-5; **1**·2Na, 139869-61-7; **1** dimethyl ester, 41204-41-5; **2**, 139869-62-8; **2**·2Na, 139869-63-9; **2** dimethyl ester, 139869-64-0; **3a**, 139869-65-1; **3a**·2Na, 139869-66-2; **3b**, 139895-04-8; **3b**·2Na, 139869-67-3; **3c**, 139869-68-4; **3c**·2Na, 139869-69-5; **3d**, 139869-70-8; **3d**·2Na, 139869-71-9; **3e**, 139869-72-0; **3e**·2Na, 139869-73-1; **3f**, 139869-74-2; **3f**·2Na, 139869-75-3; **3g**, 139869-76-4; **3g**·2Na, 139869-77-5; **4**, 139869-78-6; **4**·2Na, 139869-79-7; **5a**, 61574-53-6; **5b**, 139869-80-0; **5c**, 139869-81-1; **5d**, 51513-56-5; **5e**, 139869-82-2; **5f**, 139869-83-3; **5g**, 139869-84-4; **6a**, 139869-85-5; **6b**, 139869-86-6; **6c**, 139869-87-7; **6d**, 139869-88-8; **6e**, 139869-89-9; **6f**, 139869-90-2; **6g**, 139869-91-3; **7**, 139869-92-4; **8**, 76881-11-3; **9**, 139869-93-5; $CH_3(CH_2)_7I$, 629-27-6.

Supplementary Material Available: Plots of chemical shift vs amphiphile concentration and chemical shift vs (amphiphile concentration)$^{-1}$ for the disodium salts of **1–4** and for the dipotassium salt of **3e** and plots of dye absorbance vs amphiphile concentration for **3a**, **3d**, and **3f** (32 pages). Ordering information is given on any current masthead page.